

Production of submicron Al_2O_3 powders by electrochemical dissolution of aluminum in the presence of nitric acid

*S.S.Balabanov*¹, *V.V.Drobotenko*¹, *D.A.Permin*¹,
*E.Ye.Rostokina*¹, *M.S.Boldin*², *A.A.Murashev*²

¹Devyatykh Institute of Chemistry of High Purity Substances, Russian Academy of Sciences, 49 Tropinin Str., 603950 Nizhny Novgorod, Russia

²Lobachevsky State University of Nizhny Novgorod, Research and Development Institute of Physics and Technology, 23 Gagarin Ave., 603950 Nizhny Novgorod, Russia

Received June 7, 2018

A cost-effective and easily scalable method for the synthesis of ultrapure submicron alumina powders with a narrow particle size distribution and high sinterability is proposed. Aqueous solutions of aluminum hydroxide nanoclusters obtained by AC electrochemical dissolution of aluminum metal in the presence of nitric acid were used as a precursor. Hot pressing and vacuum sintering were used to evaluate the possibility of obtaining Al_2O_3 optical ceramics from synthesized powders.

Keywords: Alumina, fine powder, sintering, electrochemical dissolution, ceramics.

Предложен экономически эффективный и легко масштабируемый метод синтеза особо чистых субмикронных порошков оксида алюминия, имеющих узкое распределение частиц по размерам и высокую спекаемость. В качестве прекурсора использованы растворы нанокластеров гидроксидов алюминия, полученные методом электрохимического растворения металлического алюминия переменным током промышленной частоты в водном растворе азотной кислоты. Горячее прессование и вакуумное спекание использовано для оценки возможности получения оптической керамики Al_2O_3 из порошков.

Отримання субмікронних порошків Al_2O_3 електрохімічним розчиненням алюмінію в присутності азотної кислоти. *С.С.Балабанов, В.В.Дроботенко, Д.А.Пермін, Е.Е.Ростокіна, М.С.Болдін, А.А.Мурашев.*

Запропоновано економічно-ефективний метод синтезу особливо чистих субмікронних порошків оксиду алюмінію, що легко масштабується. Порошки мають вузький розподіл частинок за розмірами та високу здатність до спікання. В якості прекурсору використано розчини нанокластерів гідроксидів алюмінію що отримані методом електрохімічного розчинення металевго алюмінію змінним струмом промислової частоти у водному розчині азотної кислоти. Для оцінки можливості отримання оптичної кераміки Al_2O_3 з синтезованих порошків використано метод гарячого пресування і вакуумного спікання.

1. Introduction

Alumina ceramics are widely used in various fields of industry and technology due to high mechanical strength, wear and chemical resistance, and thermal conductivity, etc.

The properties of such ceramics are largely determined by the characteristics of the initial powders: impurity content, morphology, particle size distribution, agglomeration degree, etc. The structural-morphological characteristics of the initial powder

must be precisely controlled to obtain a material with the desired properties. Known industrial methods for producing alumina by processing bauxites do not allow the obtaining of powders with the required purity and dispersity degree that are suitable for the production of high-quality oxide ceramics. A number of studies have reported the fabrication of high quality submicron alumina powders such as mechanical, electrochemical synthesis, vapor phase reaction, sol-gel, combustion, hydrothermal, co-precipitation methods [1–5], etc. There are some limitations in all aforementioned methods.

The electrochemical method can be an alternative to existing approaches for the production of alumina powders for transparent ceramics. For example, compared to the conventional alkoxide approach, the electrochemical method does not require the use of volatile flammable organic substances and special equipment that protects aluminum alkoxides from hydrolysis by air moisture, and is cost-effective in production. Meanwhile, the method allows obtaining powders with specified and reproducible characteristics (morphology, particle size distribution, etc.) because of the possibility of regulating the electrolysis process parameters. Papers [6–9] have reported on the production of alumina submicron powders by electrochemical dissolution of aluminum in water in the presence of salts (NH_4Cl , NaCl , Na_2CO_3 , etc.) as electroconductive additives. The necessity of washing aluminum hydroxide from electrolytes increases the laboriousness of the synthesis process, and the long presence of a precipitate in the solution leads to the agglomerates formation as a result of recrystallization processes. This causes the multimode alumina particles size distribution, bulk density fluctuations, and appearance of porosity in the final products. The authors of the papers do not report on the production of transparent ceramics using electrochemically derived powders.

As shown in [10], the formation of flat $[\text{Al}_{13}(\mu_3\text{-OH})_6(\mu_2\text{-OH})_{18}(\text{H}_2\text{O})_{24}](\text{NO}_3)_{15}$ nanoclusters is observed during the electrolysis of an aluminum nitrate aqueous solution. These clusters (Al_{13}) are versatile precursors for large-scale preparation of Al_2O_3 thin films and nanoparticles for electronics, catalysis, and corrosion prevention. Similar nanoclusters can be obtained via stoichiometric dissolution of bulk $\text{Al}(\text{OH})_3$ in HNO_3 [11]. However, in both cases, the initial substances used (aluminum nitrate or aluminum hydroxide) are more expensive

(in an ultrapure state) than the target product — an ultrapure aluminum oxide obtained by other methods. AC electrolysis of aluminum metal in an aqueous solution of nitric acid can be an alternative to existing approaches because it enables carrying out the direct synthesis of aluminum hydroxide nanoclusters by a cost-effective method from industrially produced ultrapure reagents.

In the present work, we report on the successful fabrication of ultrapure submicron alumina powders with a narrow particle size distribution that are suitable for the production of transparent Al_2O_3 ceramics by electrochemical dissolution of aluminum metal in an aqueous solution of nitric acid to form aqueous aluminum hydroxide nanoclusters.

2. Experimental

Aluminum metal (99.99 % purity), nitric acid (HNO_3 , 99.999 %) and deionized water with a specific resistance of $18 \text{ M}\Omega\cdot\text{cm}$ were used as the starting materials in the present work.

Electrochemical dissolution of aluminum was carried out as follows. The plates of aluminum metal, 10–15 mm thick, were placed in a beaker with 715 ml of an aqueous solution of nitric acid with a concentration of 2.57 mol/L so that the electrodes with an area of 150 cm^2 were immersed in the electrolyte at a distance of 15–20 mm from each other. The surface of the electrodes was previously cleaned by boiling them in nitric acid solution (0.1 mol/L), followed by washing with deionized water. The electrochemical dissolution of aluminum was carried out under the action of an industrial frequency current 50 Hz through a step-down transformer at a temperature not exceeding 90°C while monitoring the current and time of the current transmission (at about 15 h) through the electrolyte until the amount of electricity passed through the electrolyte was equal to about 280 kC per mole of nitric acid.

As a result, 600.5 g of an aqueous solution of aluminum hydroxide nanoclusters of the gross-composition $\text{Al}_x(\text{OH})_{3x-y}(\text{NO}_3)_y \cdot n\text{H}_2\text{O}$, where $0.8 < x/y \leq 1$, were obtained. The concentration of the solution was determined by the thermogravimetric method after drying an aliquot and the subsequent calcining of the sample at 1300°C for 20 min, which was 15 wt.% in terms of Al_2O_3 .

Prepared transparent aqueous solution of aluminum hydroxide nanoclusters was dried in a SNOL 20/300 oven at $110\text{--}150^\circ\text{C}$ for 3 h to form xerogel. The obtained xerogel

was planetary ball milled for 10 min using high pure alumina balls and screened through a 300 mesh sieve. The resulting powder was then calcined in a laboratory furnace SNOL 6.7/1300 at different temperatures. The powders were additionally milled in a 2" Sturtevant Micronizer (Sturtevant, USA) jet mill to break of the agglomerates formed as a result of heat treatment.

To obtain ceramics, the powder, milled and calcined at 800°C, was consolidated by hot pressing and vacuum sintering. For hot pressing, pre-shaped powder was loaded into the Ø13 mm graphite mold, heated up to 1450°C with a heating rate of 20°C/min and held for 1 h before cooling down. The residual pressure in the chamber was about 10 Pa. The load was applied at the temperature of 700°C, and then increased to about 45 MPa at 40 min. Pressure was released before free cooling of the furnace. For vacuum sintering, the powder was uniaxially pressed under 250 MPa. The green bodies were annealed at 1250°C for 0.5 h in air. Ceramics were sintered at 1780°C for 3 h under a vacuum (10^{-3} Pa) at a heating rate of 5°C/min. In both cases, 500 ppm magnesia was used as a sintering aid. Finally, the samples were mirror polished on both surfaces.

X-ray diffraction analysis (XRD) of powders was done on an Ultima IV (Rigaku, Japan) X-ray diffractometer (CuK α radiation, $\lambda = 1.5406$ Å). XRD was carried out in a range of angles $2\theta = 20-80^\circ$ with a step of 0.05° , and an accumulation time of 1 s. Thermal analysis was done through methods of thermogravimetry (TG) and differential scanning calorimetry (DSC) using a Netzsch STA 409 PC/PG thermal analyzer (Netzsch, Germany). The samples were enclosed in platinum crucibles, and the measurements were conducted in an argon flow at a heating rate of 10 K/min up to a temperature of 1150°C. The impurity composition of the aqueous solution of aluminum hydroxide nanoclusters and Al₂O₃ powders was determined by inductively coupled plasma atomic emission spectroscopy (ICP-AES) using the iCAP6300 (Thermo scientific, USA). Measurements of particle size distribution were carried out by NanoBrook 90Plus Zeta (Brookhaven Instr. Corp., USA) equipment using the dynamic light scattering method (DLS). Aluminum hydroxide nanoclusters were measured after passing the solution through a 0.2 μ m PTFE filter to ensure removal of residual particles. Al₂O₃ powder, before measurement, was calcined at 1150°C

for 0.5 h in air, and then dispersed in water by ultrasound. The morphology of the powder, the microstructure of ceramics, and the average grain size were studied using a metallographic microscope, MMH-2 (LOMO, Russia), and an analytical scanning electron microscope (SEM), JSM-6390LA (JEOL, Japan), using the imaging of back-scattered electrons and secondary electrons. The kinetics of the alumina compacts densification was investigated using a NETZSCH DIL 402C dilatometer (Netzsch, Germany) at a heating rate of 5°C/min, at temperatures up to 1615°C and high vacuum.

3. Results and discussion

It is known from [7–9] that the electrochemical dissolution of aluminum metal using NH₄Cl, NaCl, NaOH, Na₂CO₃, NaNO₃, etc., as electroconductive additives leads to the formation of a bulk precipitate of aluminum hydroxide or oxide, which is subsequently washed from the electrolyte, dried and calcined at various temperatures. The need for additional processing of aluminum hydroxide (washing away from the electrolyte ions and, especially, from the sodium cation, etc.) complicates the possibility of obtaining pure nanodisperse or submicron powder. Increasing productivity and scaling up of such process is a complex task.

The formation of an aluminum hydroxide/oxide precipitate in the dissolution of aluminum does not occur when nitric acid is used as an electroconductive additive and the certain synthesis conditions are met. Transparent solutions of aluminum hydroxide nanoclusters of the approximate composition $Al_x(OH)_{3x-y}(NO_3)_y \cdot nH_2O$, where $0.67 \leq x/y < 1.33$, are formed when the amount of electricity passed through the electrolyzer is 190–390 kC per mole of nitric acid. According to the DLS results, the nanoclusters size is in the range of 1.8–3.5 nm with a maximum in the region of 2 nm. A complex with lower aluminum content up to the formation of aluminum nitrate is formed when less electricity is passed through the electrolyte. This leads to a decrease in the aluminum concentration in the solution, a decrease in the productivity of the process, and an increase in the amount of nitrogen oxides released upon calcination of the dried complexes. When more than 390 kC electricity is passed through the electrolyte, solutions of aluminum hydroxide nanoclusters with a higher aluminum content, $Al_x(OH)_{3x-y}(NO_3)_y \cdot nH_2O$, where $x/y > 1.33$, are formed. Such solutions

are coagulated with the release of the precipitate at an elevated temperature or under the action of an electric current. The possibility of obtaining such complexes was previously established as a result of the dissolution process with the necessary amount of nitric acid of amorphous aluminum hydroxide obtained from crystalline aluminum alkoxide [12, 13].

Maintaining the high purity of the product is one of the major advantages of using an aqueous solution of aluminum hydroxide nanoclusters compared to commercial aluminum salts. Thus, the impurity composition of the aqueous solution of the complex is almost entirely related to the purity of the initial reagents, which are produced in a ultrapure state on an industrial scale (the metal impurities content is at level of ppm or less); on the contrary, the industrially produced aluminum salts need to be subjected to additional purification. The cost-effectiveness of use of aluminum hydroxide nanoclusters is achieved due to the lower content of nitrate anions compared to aluminum nitrate, as well as the higher concentration of aluminum ions in the solution (at least twice as high compared to aluminum salts). The reproducibility of the aluminum hydroxide nanoclusters solution's characteristics is provided by easily controlled parameters — the solution temperature, the quantity of electricity, and the acid concentration.

Table shows the results of the ICP-AES analysis of the impurity composition of aluminum hydroxide nanoclusters solution and Al_2O_3 powder for a wide range of impurities. As is known, impurities have a strong effect on the final characteristics of ceramics. For example, it reduces the hardness and fracture strength of the material, concentrating on the grain boundaries. "Coloring" impurities (usually transition metals) reduce transmission of material at certain wavelengths. In addition, a number of elements and their compounds change the sinterability of powders, which also affects the final characteristics of ceramics. In general, the initial powder purity of 99.99+ wt. % is required for obtaining the majority of functional ceramics (for example, optically transparent). As can be seen from Table, the impurity content in the samples does not exceed the allowable values, which meets the requirements for optical ceramics precursors. The 550 ppm magnesium was added as a sintering additive. It can be seen that the initial solution contains a small amount of Mg.

Table. Impurity composition of aluminum hydroxide nanoclusters solution and Al_2O_3 powder determined by ICP-AES method

Impurity	Impurity content, ppm	
	Aluminum hydroxide nanoclusters solution	Al_2O_3 powder
Ca	0.2	2.0
Cd	<0.02	<0.2
Ce	<0.03	<0.3
Co	0.14	2.1
Cr	0.02	2.5
Cu	0.3	1.7
Dy	<0.01	<0.3
Er	<0.06	<0.7
Eu	<0.07	<0.5
Fe	0.9	6.8
Gd	<0.04	<0.7
Hf	<0.05	<0.5
Ho	<0.05	<0.7
K	0.15	3.1
La	<0.02	0.2
Lu	<0.04	<0.3
Mg	2.0	550
Mn	0.06	0.5
Mo	<0.01	<0.1
Na	0.95	5.2
Nb	<0.01	<0.1
Nd	<0.3	<2
Ni	<0.2	2.0
Pb	<0.5	<5
Pr	<0.1	<5
Si	<3.0	<50
Sm	<0.5	<8
Sn	<0.05	<0.5
Tb	<0.2	<2
Ti	≤0.02	0.7
Tm	<0.03	<0.3
V	<0.8	<3
W	<0.05	<0.5
Y	0.1	1.7
Yb	<0.002	<0.05
Zn	0.12	1
Zr	<0.01	<0.1

Relative standard deviation of the analy-

Fig. 1 shows the XRD patterns of the alumina powders after calcination at 800 and 1250°C. For the 800°C powder, the observed peaks are strongly broadened due to low crystallite sizes and low crystallinity. The size of the coherent-scattering region determined from 100 % intensity peak is 26.4(7) Å. The positions of peaks in accord-

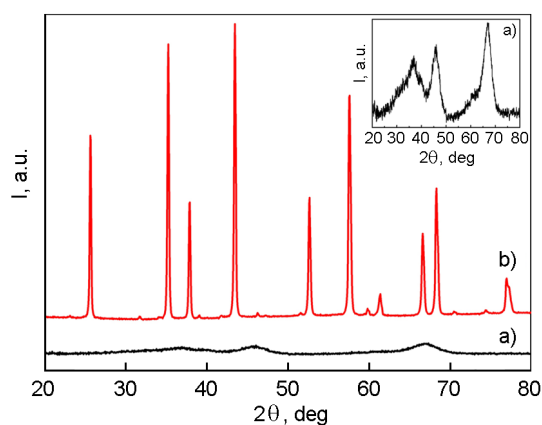


Fig. 1. XRD patterns of the alumina powder after annealing at 800°C (a) and 1250°C (b) for 30 min.

ance with the theoretical X-ray reflections are most characteristic for cubic alumina ($\text{Al}_2\text{O}_{2.985}$), a unit cell dimension of 7.9110 Å. However, the identification of a particular polymorphic modification of alumina and determining of quantitative phases content cannot be carried out unambiguously because of the strong amorphization of the sample. It appears that the sample consists of a mixture of so-called transition alumina phases, presumably γ - or η -modifications. Crystallization of γ - or η - Al_2O_3 was made possible by growing from nucleation centers in an amorphous matrix. A similar pattern was observed for the alumina powders prepared from $[\text{Al}_{13}(\mu_3\text{-OH})_6(\mu_2\text{-OH})_{18}(\text{H}_2\text{O})_{24}(\text{NO}_3)_{15}]$ [11], as well as by the sol-gel, combustion and other methods [14, 15]. The structures of these transition aluminas are traditionally considered to be based on a face-centered cubic (FCC) array of oxygen anions. The structural differences between these forms only involve the arrangement of aluminum cations in the interstices of an approximately cubic close-packed array of oxygen anions [16]. The degree of crystallinity was improved by increasing the temperature. Transformation of the transition aluminas to the final thermodynamically stable α -alumina takes place at temperatures above 1100°C. The XRD pattern of the sample calcined at 1250°C was typical for α - Al_2O_3 , the size of coherent-scattering region is 40 nm.

Differential scanning calorimetric and thermogravimetric curves of the dried aluminum hydroxide nanoclusters solution (xerogel) are shown in Fig. 2. As can be seen from Fig. 2, the most weight loss (about 54 %) occurs up to 400°C due to the evaporation of adsorbed and chemically

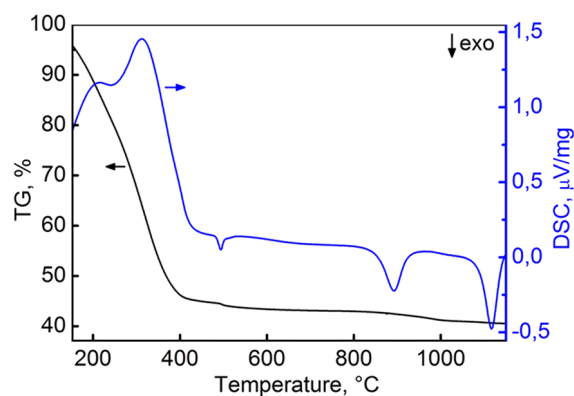


Fig. 2. TG-DSC curves of the dried aluminum hydroxide nanoclusters solution (xerogel).

bonded water, as well as the decomposition of nitrate groups of the precursor, which is accompanied by two endothermic peaks with maxima at about 215 and 313°C, respectively, on the DSC curve. The small exothermic peak at 494°C on the DSC curve may be associated with the crystallization of alumina of γ - or η -modifications. This transformation is accompanied by a tiny weight loss (about 0.7 %) on the thermogravimetric curves. In the range of 800–1000°C, the $\gamma(\eta)$ - Al_2O_3 is converted to θ -alumina, which is accompanied by a corresponding exothermic peak with a maximum of about 892°C and a small mass loss (about 2 %) on the TG-DSC curves. The exothermic peak at 1117°C corresponds to the crystallization of the α - Al_2O_3 phase, which was also confirmed by results of XRD analysis as shown above.

Fig. 3 shows SEM micrographs of the alumina powders after annealing at 1150°C and grinding in a jet mill. The powder consists of rounded shape primary particles with an average size of about 400 nm. The primary particles of powders were combined into weakly agglomerated secondary particles reaching up to 1–2 μm in size.

Fig. 4 illustrates the DLS histograms of particle size distribution of the alumina powder depending on the ultrasonication time. The as-prepared powders (without sonication) are mainly composed of particles from 0.5 to 1.4 μm in size. Even a short ultrasonic dispersing of the powder suspensions causes decreases in an average particle size. After dispersing for 15 min, the powder shows a narrow particle size distribution, with peak centered at 394 nm, which is consistent with SEM data. The destruction of particle aggregates at ultrasonic processing additionally confirms the as-

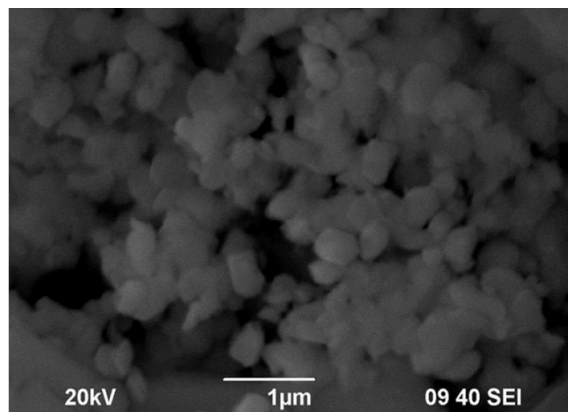


Fig. 3. Scanning electron micrographs of the alumina jet milled powder after heat treatment at 1150°C for 0.5 h.

sumption that the obtained alumina powders consist of "soft" agglomerates. Comparison of the sizes of primary particles (at about 400 nm) and coherent-scattering region (40 nm) indicates their polycrystalline structure.

Fig. 5 shows a shrinkage curve and its derivative for the calcined at 800°C and milled magnesia-doped Al_2O_3 powders compacts. An intensive change of the shrinkage rate of the sample begins at 1000°C. The shrinkage process takes place in two stages with maximum speeds at 1090 and 1400°C, respectively. Within the temperature range 1000–1160°C, the formation of the stable α -alumina phase from transition aluminas takes place, which leads to a first linear shrinkage of about 12 %. Such a significant volume change of the sample during the "transition aluminas \rightarrow alpha alumina" phase transformation is due to the crystallographic structure change from cubic face centered towards a compact hexagonal structure and activation of the sintering process by that transformation. For temperatures higher than 1200°C, shrinkage due to densification of the resultant α - Al_2O_3 phase is observed. The linear shrinkage of the sample continues to a temperature of about 1500°C, after which the shrinkage rate begins to decrease.

To estimate the possibility of obtaining optical ceramics, the consolidation of alumina powders was carried out by vacuum sintering and hot pressing. In both cases, ceramics with density of more than 99 % of theoretical value were obtained. Fig. 6 shows micrographs of Al_2O_3 ceramics — the fractured surface of hot-pressed sample and chemically etched polished surface of vacuum sintered sample. The hot-pressed ceramics have a dense microstructure; the av-

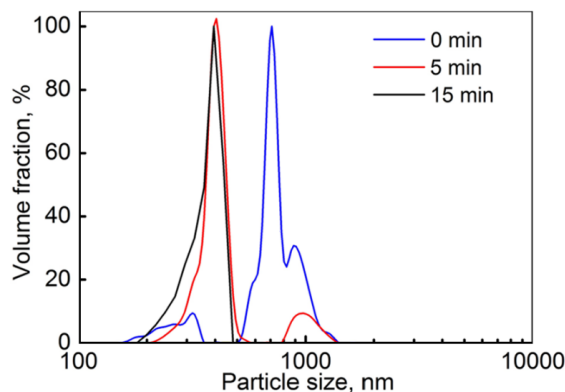


Fig. 4. Particle size distribution of the alumina jet milled powder after heat treatment at 1150°C for 0.5 h at ultrasonication for 0.5 and 15 min.

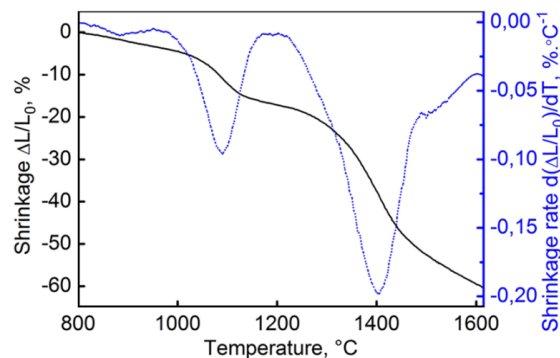


Fig. 5. Shrinkage (solid lines) and shrinkage rate (dotted lines) curves of the powder compacts of alumina.

erage grain size is 550 nm. Individual pores up to 200 nm in size are visible at triple points and at grain boundaries. The vacuum sintered ceramics also have a dense microstructure; the average grain size is 7 μm . In the sample, there are both separate isolated pores and pores at triple points up to 2 μm in size.

Fig. 7 shows the in-line transmittance (ILT) spectra of ceramics in the infrared wavelength range. We associate the lower transmission of ceramics compared to sapphire, as well as the difference in the transmission spectra of ceramics with each other, with both the residual porosity and birefringence (due to the hexagonal structure of α - Al_2O_3). Submicron grain size of the hot-pressed ceramics provides maximum scattering in the visible wavelength range, whereas vacuum sintered ceramics have a maximum scattering in the infrared range. In addition, low temperature and short sintering time during hot pressing lead to predominantly submicron pores formation. The ceramics were almost completely opaque in a visible wavelength range due to the con-

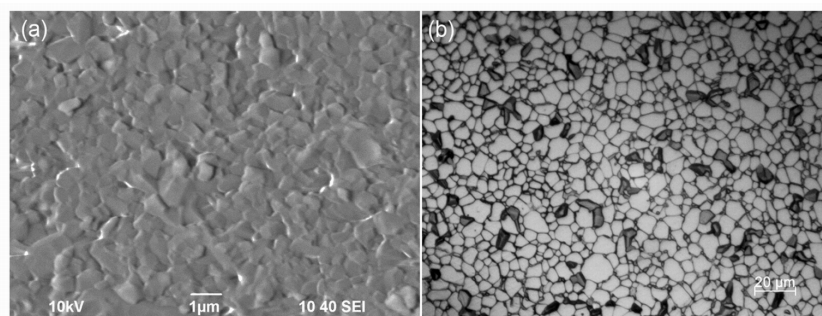


Fig 6. Micrographs of Al_2O_3 ceramics – the fractured surface of hot-pressed sample (a) and chemical-lyetched polished surface of vacuum sintered sample (b).

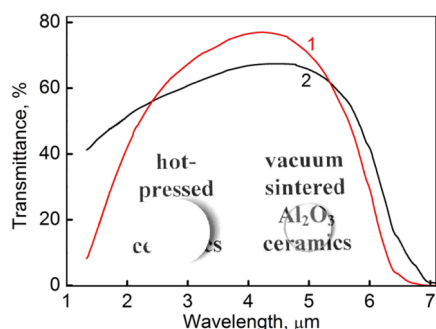


Fig. 7. Optical in-line transmission spectra of hot-pressed 1.5 mm thick (1) and vacuum sintered 0.8 mm thick (2) Al_2O_3 ceramic samples. Inset — the photo of Al_2O_3 ceramics.

tent of submicron pores, but the light transmission in the IR range attained 77 %. Although vacuum sintering provides a relatively lower residual porosity, non-optimal modes of powder compaction and subsequent sintering cause not only the healing of pores, but also their consolidation. In this regard, but the pore size distribution is shifted to the micrometer range, which leads to an increase of long-wave radiation scattering, but to a lesser extent affects the transparency in the visible wavelength range.

As shown by experiments, alumina powders obtained from aluminum hydroxide nanoclusters solutions have high sinterability and are suitable for producing optical ceramics. Further optimization of the compaction and sintering modes is necessary to increase the transparency of ceramics.

4. Conclusions

A cost-effective and easily scalable method for the synthesis of aluminum hydroxide nanoclusters by AC electrochemical dissolution of aluminum metal in an aqueous solution of nitric acid is proposed. Ultrapure submicron (400 nm) alumina powders with a narrow particle size distribution and high sinterability from aluminum hy-

droxide nanoclusters solutions was successfully fabricated. Al_2O_3 ceramics, having in-line transmission up to 77 % at the 4–5 μm wavelength range (for 1.5 mm-thick sample) and average grain size 550 nm, was obtained by hot pressing. The ceramics obtained by vacuum sintering were transparent both in visible and IR wavelength range.

Acknowledgment. This research was supported within the frame of the program of fundamental scientific research of the state academies of sciences for 2013-2020 (project No. 0095-2016-0016).

References

1. Y.Wu, Y.Zhang, X.Huang, J.Guo, *Ceram. Int.*, **27**, 265 (2001).
2. M.L.Panchula, J.Y.Ying, *Nanostructured Mater.*, **9**, 161 (1997).
3. V.D.Zhuravlev et al., *Ceram. Int.*, **39**, 1379 (2013).
4. J.Li, Y.Pan, C.Xiang et al., *Ceram. Int.*, **32**, 587 (2006).
5. P.K.Sharma, M.H.Jilavi, D.Burgard et al., *J. Am. Ceram. Soc.*, **81**, 2732 (2005).
6. S.Woo, J.-H.Park, C.K.Rhee et al., *Microelectron. Eng.*, **89**, 89 (2012).
7. A.F.Dresvyannikov, E.V.Petrova, M.A.Tsyganova, *Russ. J. Phys. Chem. A*, **84**, 642 (2010).
8. V.V.Korobochkin, V.I.Kosintsev, L.D.Bystritskii, E.P.Kovalevskii, *Inorg. Mater.*, **38**, 914 (2002).
9. D.Pathania, R.Katwal, H.Kaur, *Int. J. Miner. Metall. Mater.*, **23**, 358 (2016).
10. W.Wang et al., *Proc. Natl. Acad. Sci.*, **110**, 18397 (2013).
11. B.L.Fulton et al., *Chem. Mater.*, **29**, 7760 (2017).
12. V.V.Drobotenko, S.S.Balabanov, T.I.Storozheva, *Inorg. Mater.*, **46**, 295 (2010).
13. S.S.Balabanov, E.M.Gavrishchuk, V.V.Drobotenko et al., *Inorg. Mater.*, **50**, 830 (2014).
14. M.Shojaie-Bahaabad, E.Taheri-Nassaj, *Mater. Lett.*, **62**, 3364 (2008).
15. B.Sathyaseelan, I.Baskaran, K.Sivakumar, *Soft Nanosci. Lett.*, **3**, 69 (2013).
16. J.A.Jimenez, I.Padilla, A.Lopez-Delgado et al., *Int. J. Appl. Ceram. Technol.*, **12**, E178 (2015).